Electronic Supporting Information

A π-π 3D network of tetranuclear μ_2 / $\mu_3$carbonato Dy(III) bis-pyrazolylpyridine clusters showing single molecule magnetism features.

Ian. A. Gass, Boujemaa Moubaraki, Stuart .K. Langley, Stuart. R. Batten and Keith. S. Murray*

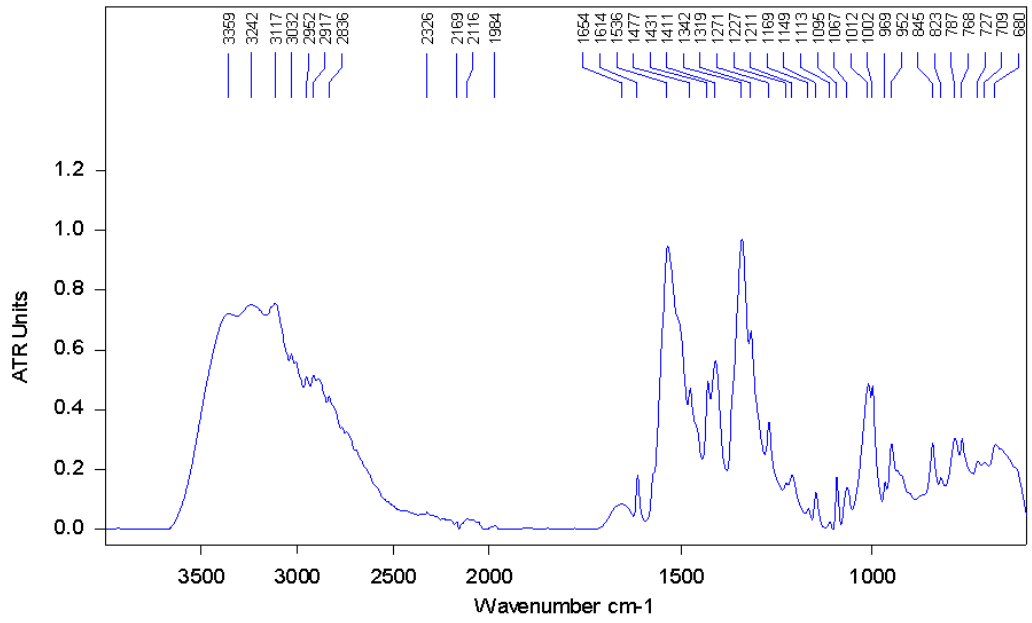

Fig. S1 ATR infrared spectra of **1** at 298K between 4000 and 600 cm^{-1}

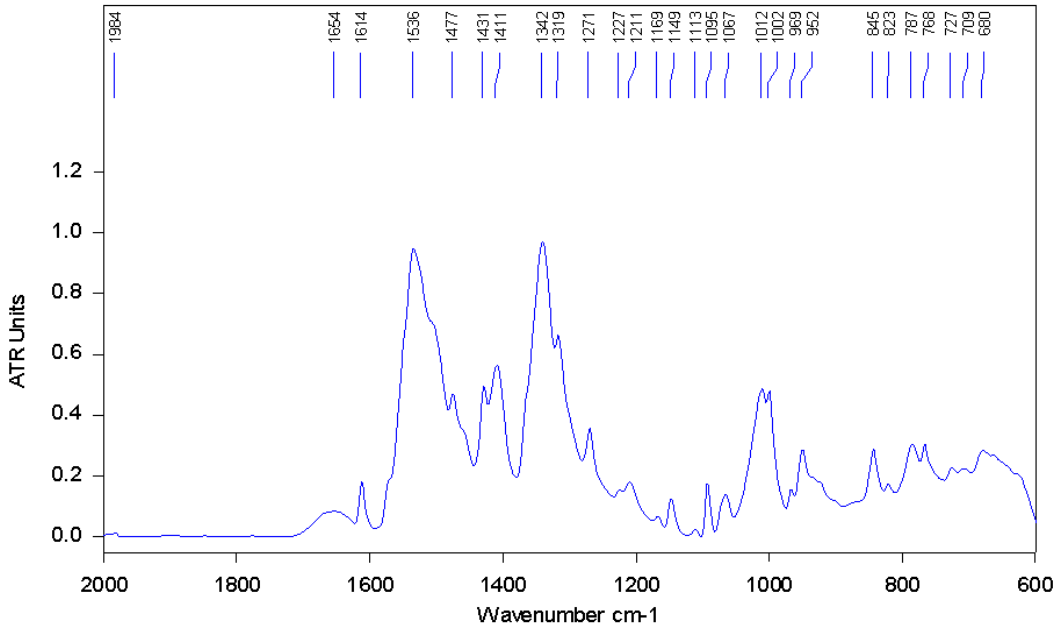

Fig. S2 ATR infrared spectra of **1** at 298K between 2000 and 600 cm^{-1}

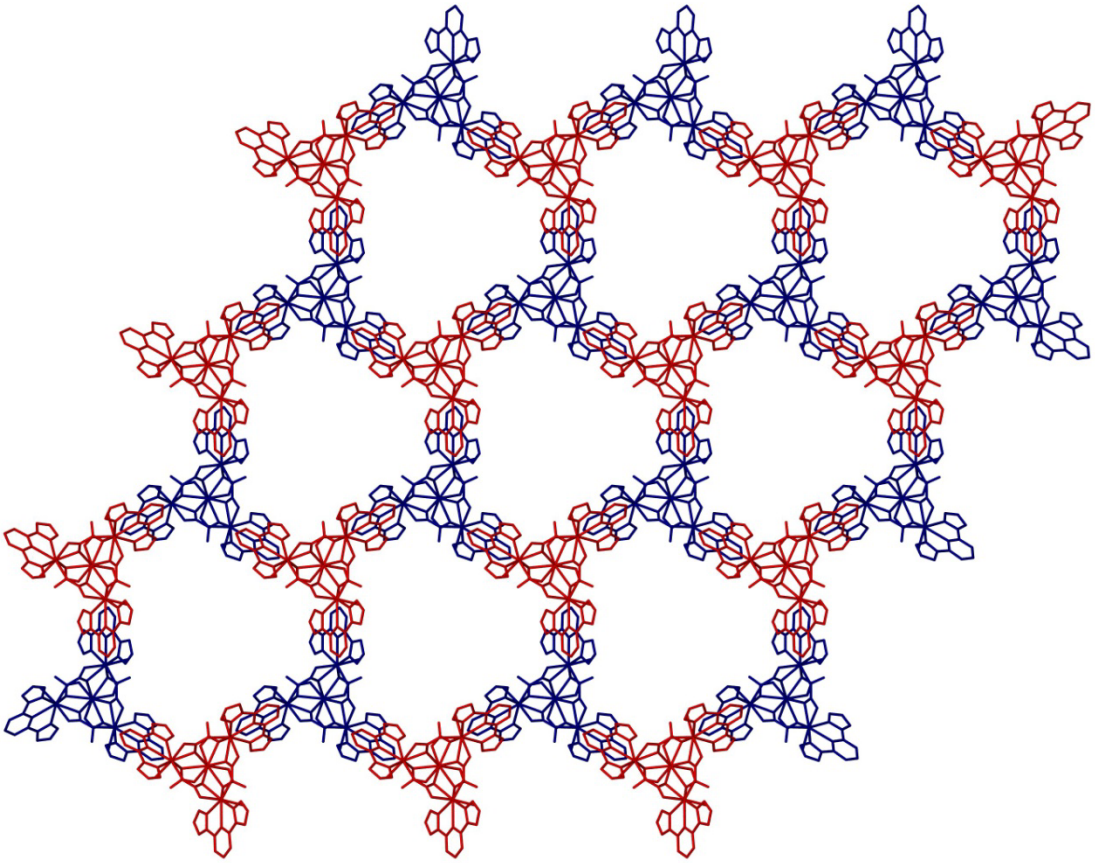

Fig. S3 X-ray crystal structure of **1** as viewed along c showing the alternating clockwise (blue) and anticlockwise (red) enantiomers. Assignment of the enantiomers orientation was made by considering the orientation of the 3-bpp ligands as viewed down the 3 fold axis with the μ_2 carbonates facing upwards.

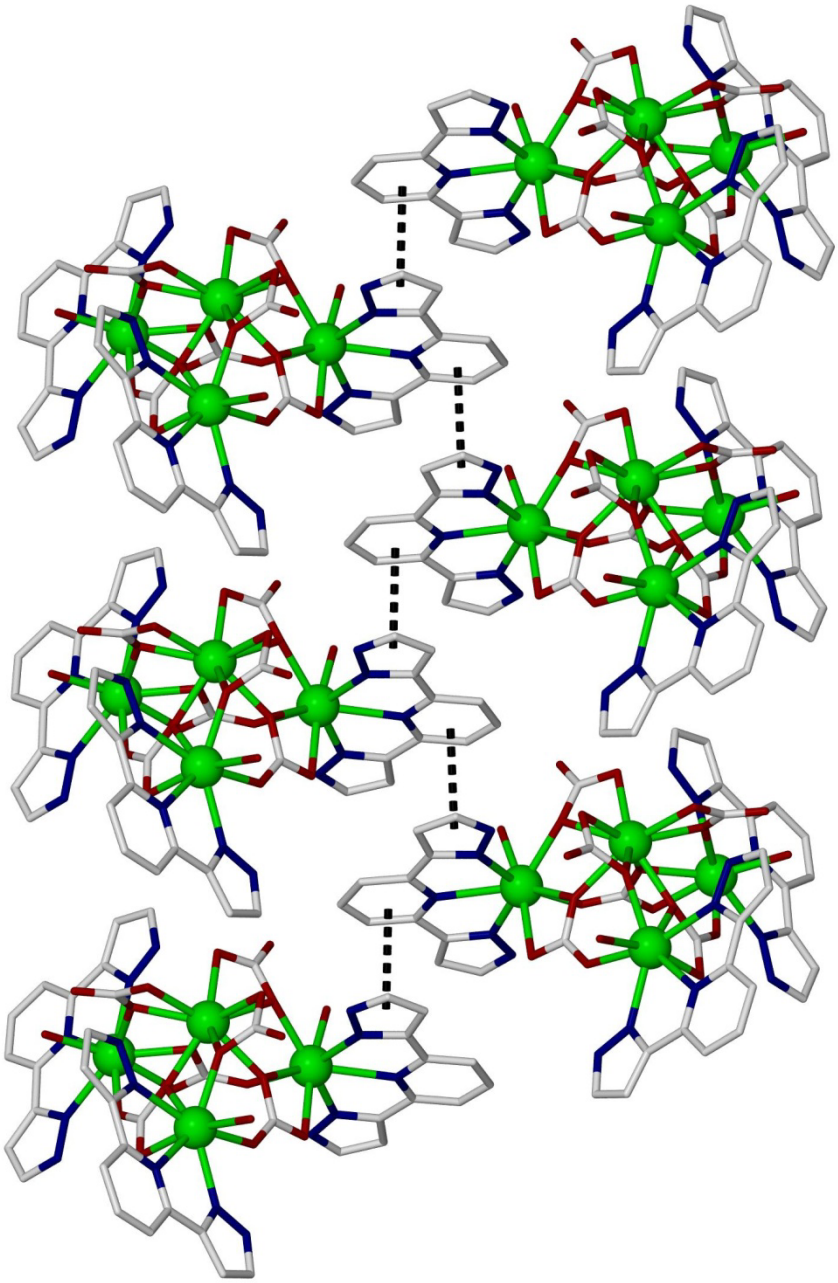

Fig. S4 View of the face to face π-π stacking interactions in **1**.

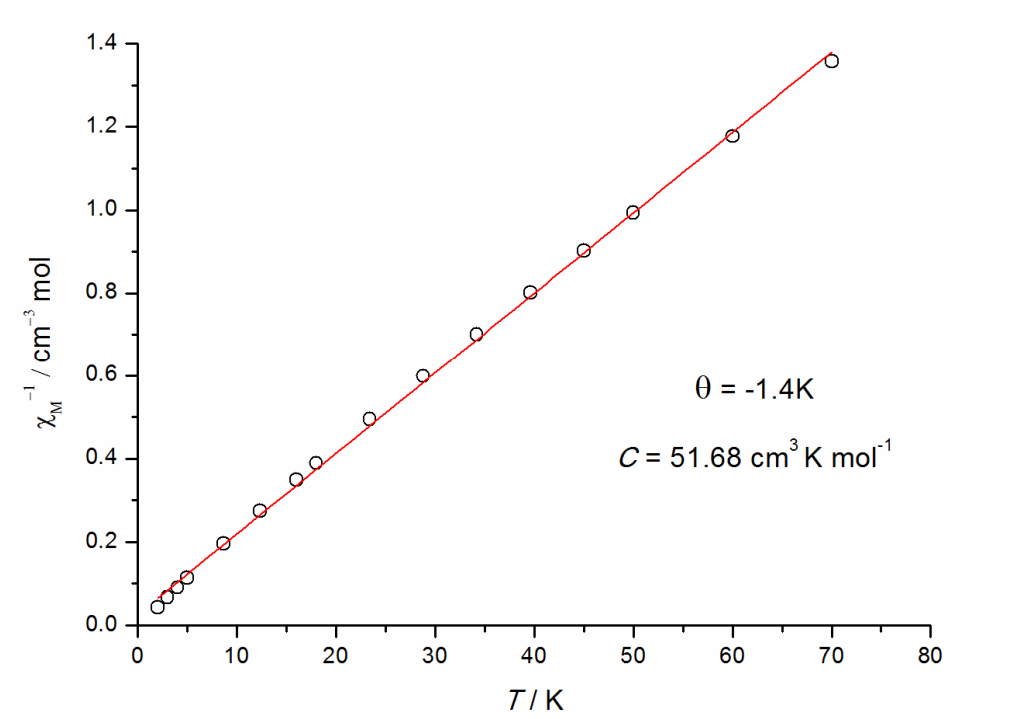

Fig. S5 Plot of χ_M^{-1} vs T for **1** at 0.088 kOe with the linear fit shown as a red line.

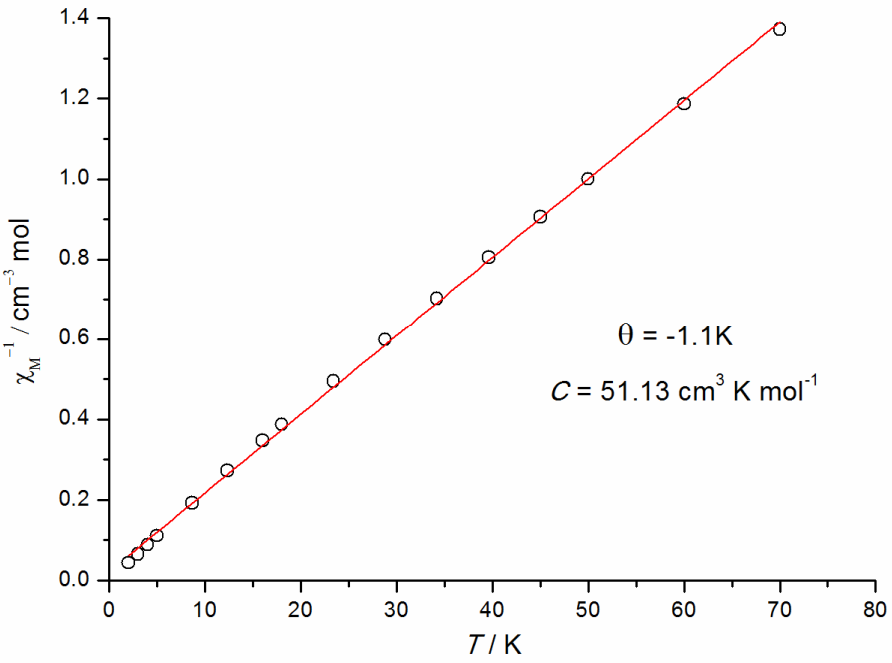

Fig. S6 Plot of χ_M^{-1} vs T for **1** at 1 kOe with the linear fit shown as a red line.

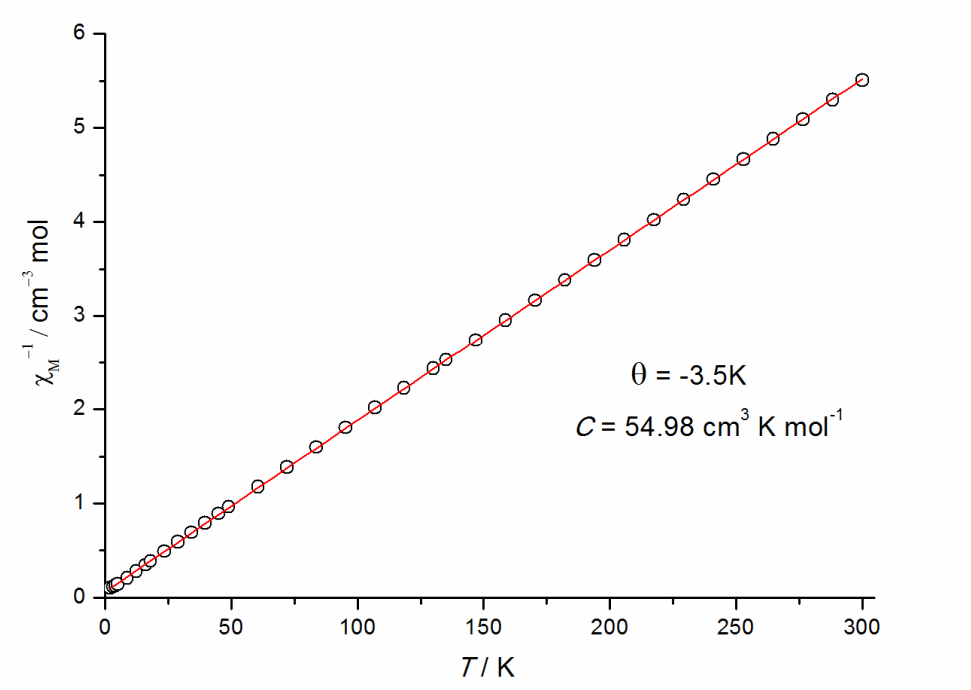

Fig. S7 Plot of χ_M^{-1} vs T for **1** at 10 kOe with the linear fit shown as a red line.

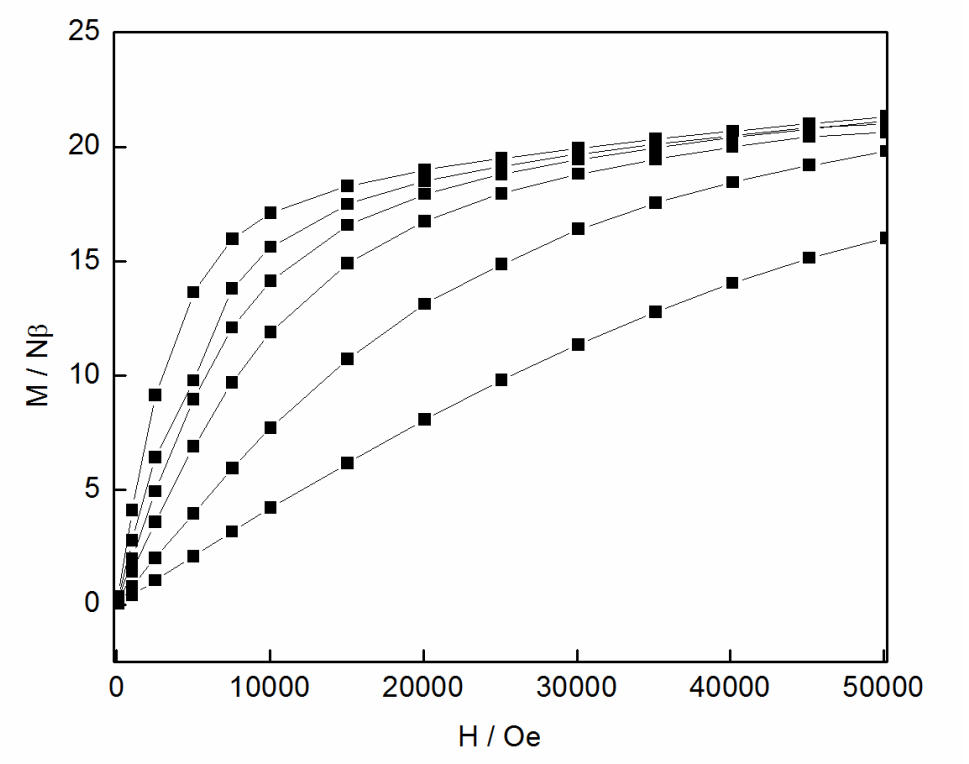

Fig. S8 *M* vs *H* isothermal plots for **1** in the 2 (top), 3, 4, 5.5, 10 and 20K (bottom) temperature range. The solid lines are guides for the eyes only.

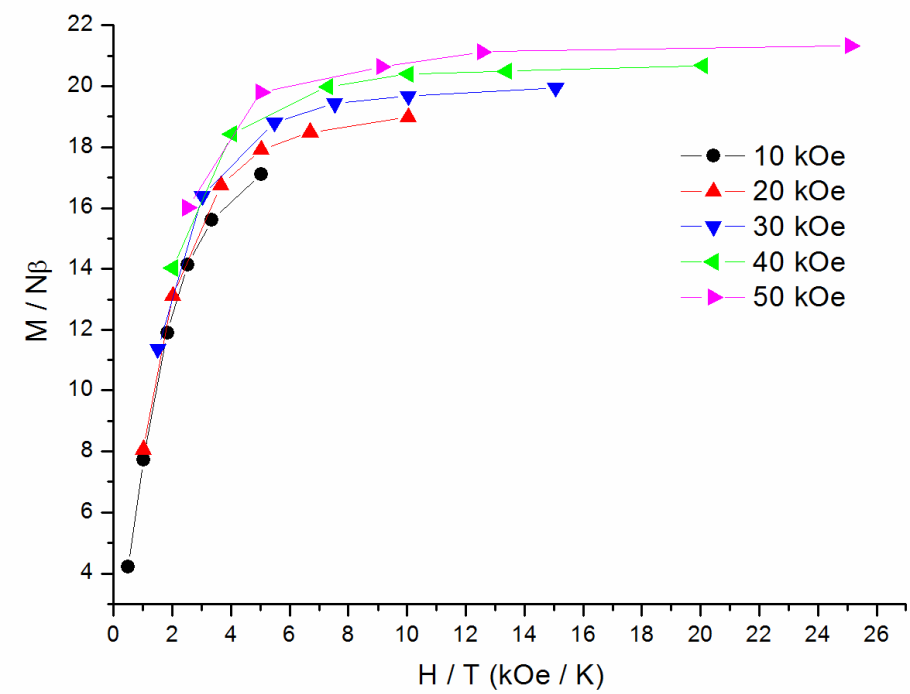

Fig. S9 Plot of reduced magnetisation *M* vs *H* / T for **1**. The solid lines are guides for the eyes only.

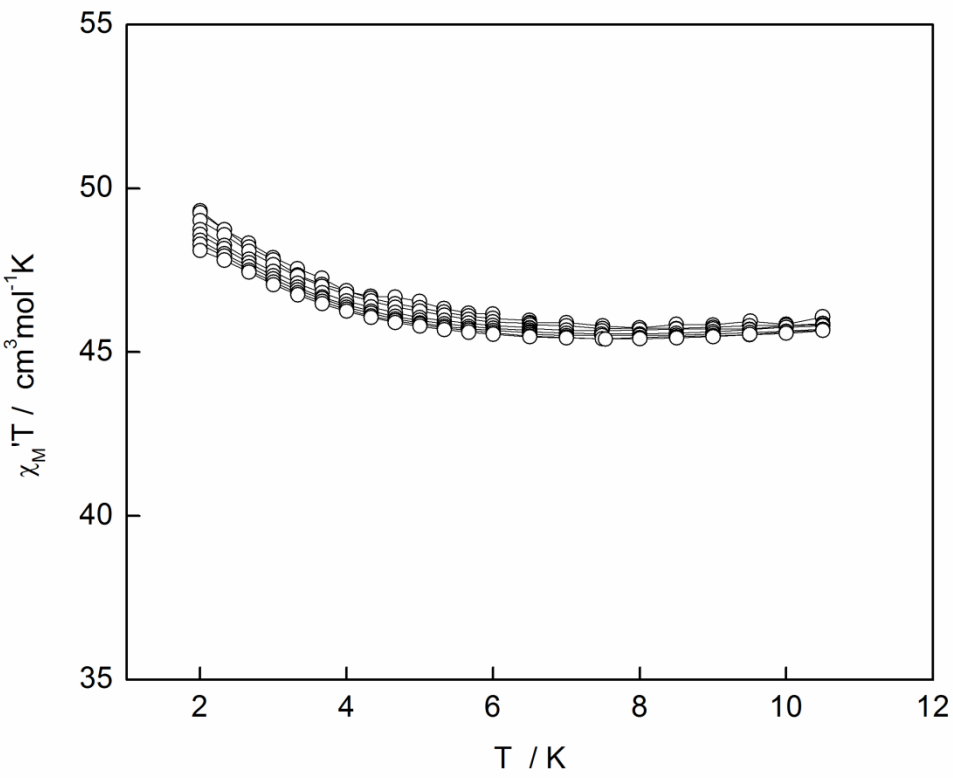

Fig. S10 Plot of $\chi'_M T$ vs T for **1** at zero applied dc field at the ac frequencies shown in Fig. 2.

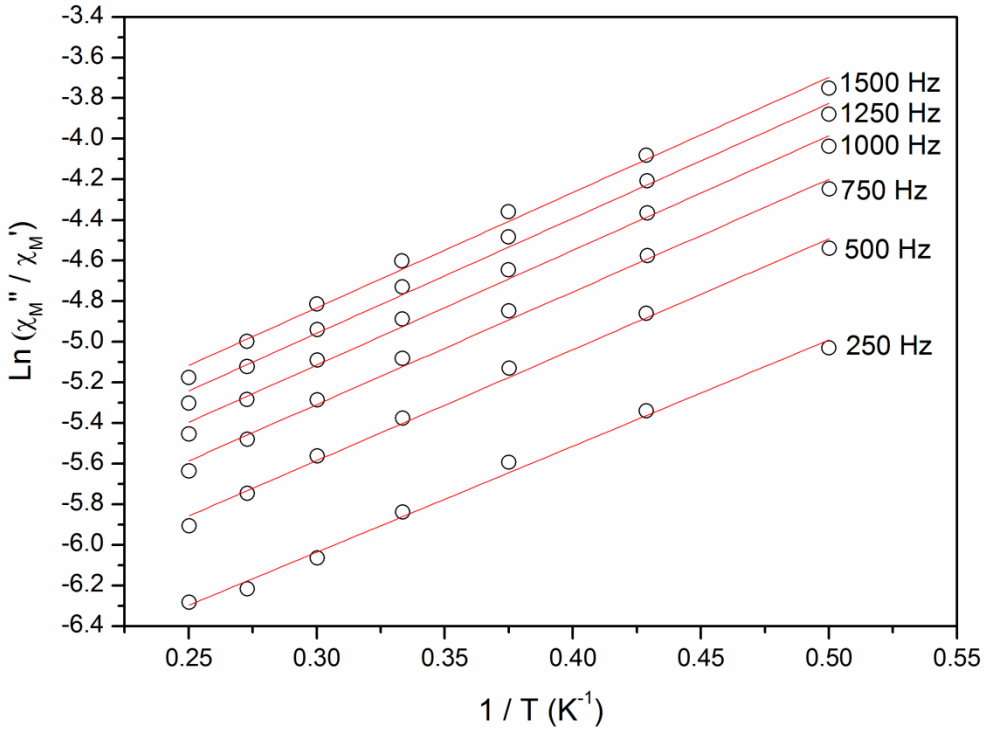

Fig. S11 Plot of ln (χ''_M / χ'_M) vs 1 / T for **1.**

E_a Estimation. By considering the relation[1]

$$\ln(\chi''_M / \chi'_M) = \ln(\omega\tau_o) + E_a/k_BT \qquad (1)$$

where χ''_M and χ'_M are the out-of-phase and in-phase components of the susceptibility, ω is the oscillating frequency of the ac experiment, τ_o is the preexponential factor of the Arrhenius law $\tau = \tau_o \exp(E_a / k_BT)$, E_a is the activation energy, k_B the Boltmann constant and T temperature we can plot ln (χ''_M / χ'_M) vs 1 / T for different frequencies whose linear fits will yield the parameters E_a and τ_o for each frequency as shown in Fig. S8. The mean of the six E_a values is 5.54 K with a standard deviation of 0.07 and the mean of the six τ_o values is 1.3 x 10^{-6} s with a standard deviation of 1.6 x 10^{-7}. These values are an estimate only but provide reasonable ballpark figures when the peaks in the χ''_M vs T plot are beyond the low temperature and high frequency limits (2K and 1500Hz) of the SQUID magnetometer used.

1. J. Bartolomé, G. Filoti, V. Kuncser, G. Schinteie, V. Mereacre, C. E. Anson, A. K. Powell, D. Prodius and C. Turta, *Phys. Rev. B.,* 2009, **B80**, 014430.

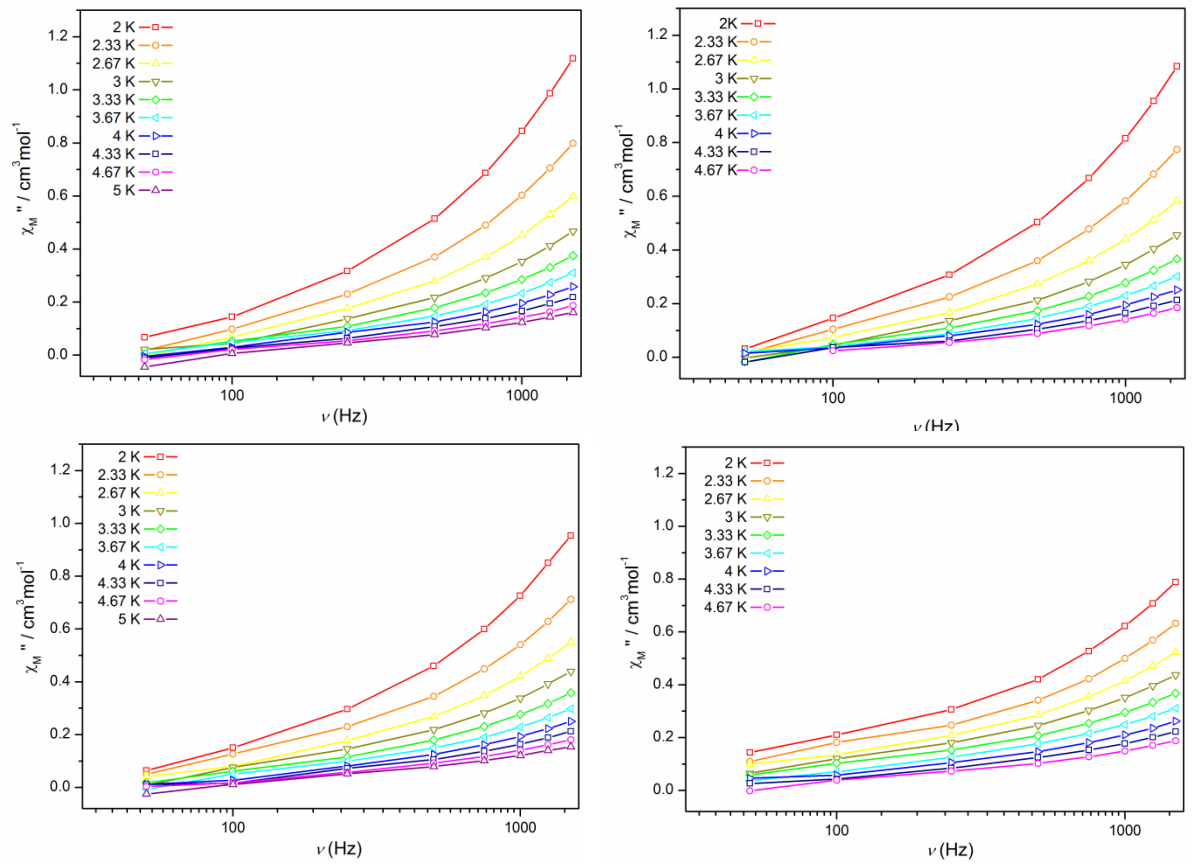

Fig. S12 Plots of χ''_M vs frequency ν for **1** at zero applied dc field (top left), 500 Oe (top right), 1500 Oe (bottom left) and 3000 Oe (bottom right).

Table S1. Bond Lengths (Å) for **1** at 123K.

Dy1-O3	2.331(4)	N1-C1	1.334(8)
Dy1-O4	2.434(4)	N2-C3	1.406(8)
Dy1-O6	2.402(4)	N3-C8	1.321(8)
Dy2-O1	2.416(4)	N3-C4	1.340(8)
Dy2-O2	2.302(4)	N4-N5	1.320(8)
Dy2-O3	2.326(3)	N4-C9	1.365(8)
Dy2-O4	2.327(4)	N5-C11	1.348(9)
Dy2-O7	2.345(4)	C1-C2	1.357(10)
Dy2-N2	2.487(5)	C2-C3	1.356(10)
Dy2-N3	2.566(4)	C3-C4	1.428(10)
Dy2-N4	2.469(5)	C4-C5	1.406(9)
O1-C12	1.270(6)	C5-C6	1.424(11)
O2-C12	1.277(6)	C6-C7	1.351(10)
O3-C12	1.307(6)	C7-C8	1.396(8)
O4-C13	1.296(7)	C8-C9	1.455(9)
O5-C13	1.250(7)	C9-C10	1.385(9)
O6-C13	1.299(8)	C10-C11	1.370(10)

Physical Measurements

Magnetic Susceptibility Measurements. Variable-temperature, solid state direct current (dc) magnetic susceptibility data down to 2K were collected with an applied fields up to of 5 T on a Quantum Design MPMS 7T SQUID magnetometer calibrated by use of a standard palladium sample (Quantum Design) of accurately known magnetization or by use of magnetochemical calibrants such as $CuSO_4 \cdot 5H_2O$. Microcrystalline samples were dispersed in Vaseline in order to avoid torquing of the crystallites. The sample mulls were contained in a calibrated capsule held at the centre of a drinking straw that was fixed at the end of the sample rod. Variable-temperature, alternating current (ac) magnetic susceptibility data down to 2K were collected with applied dc fields up to 0.3T, ac field of 3.5 Oe and frequencies up to 1500 Hz on a Quantum design PPMS.

Infrared Spectroscopy measurements were performed on the Bruker Equinox 55 diamond anvil Attenuated Total Reflection (ATR) spectrometer using Opus-6 software system.

Microanalytic analysis (C, H, N) were performed by the Campbell Microanalytical Laboratory, University of Otago, New Zealand.

General crystallographic details: To try and resolve unassignable electron density located in the channels data was collected on an Oxford Gemini Ultra diffractometer at 123(2)K with Mo-Kα radiation (λ = 0.7107 Å) and Cu-Kα radiation (λ = 1.5418 Å). In both cases there was diffuse electron density associated with badly disordered solvent in the channels which could not be modelled appropriately. SQUEEZE[2] was then applied to the collection with Mo-Kα radiation and presented here. This had the effect of markedly improving the agreement indices. **Crystal data for 1**: (CCDC 853161) $C_{39}H_{27}Dy_4N_{15}O_{21}$, M = 1691.76, colourless hexagonal prism, 0.40 x 0.10 x 0.10 mm, trigonal, space group *P*31c, a = 21.3354(3), b = 21.3354(3), c = 11.5428(3) Å, α = 90, β = 90, γ = 120°, V = 4550.33(15) Å^3, Z = 2, D_c = 1.235 g cm^{-3}, F_{000} = 1596, $2\theta_{max}$ = 55°, Oxford Gemini Ultra, Mo-Kα radiation, λ = 0.71073

Å, T = 123(2) K, 29294 reflections collected, 5892 unique (R_{int} = 0.0446). Final GoF = 1.017, R_1 = 0.0348, wR_2 = 0.0775, R indices based on 5892 reflections with $I > 2\sigma(I)$ (refinement on F^2), 238 parameters, 1 restraint. μ = 3.298 mm^{-1}.

2. A. L. Spek, *J. Appl. Crystallogr.*, 2003, **36**, 7.